Ionization Energies for the Actinide Mono- and Dioxides Series, from Th to Cm: Theory versus Experiment

Ivan Infante,*,† Attila Kovacs,‡ Giovanni La Macchia,§ Abdul Rehaman Moughal Shahi,§ John K. Gibson,|| and Laura Gagliardi*,⊥

Kimika Fakultatea, Euskal Herriko Unibertsitatea and Donostia International Physics Center (DIPC), P.K. 1072, 20080 Donostia, Euskadi (Spain), Research Group for Materials Structure and Modeling of the Hungarian Academy of Sciences, Budapest University of Technology and Economics, H-1111 Budapest, Szt. Gellért tér 4, Hungary, Department of Physical Chemistry, University of Geneva, 30 Quai Ernest Ansermet, CH-1211 Geneva, Switzerland, Chemical Sciences Division, Lawrence Berkeley National Laboratory, Berkeley, California 94720, USA, and Department of Chemistry, University of Minnesota and Supercomputing Institute, 207 Pleasant St. SE, Minneapolis, Minnesota 55455, USA

Received: February 23, 2010

The results of a computational study with multiconfigurational quantum chemical methods on actinide monoxides (AnO) and dioxides (AnO_2) for An = Th, Pa, U, Np, Pu, Am, and Cm, are presented. First and second ionization energies were determined and compared with experimental values, when available. The trend along the series is analyzed in terms of the electronic configurations of the various species. The agreement with experiment is excellent in most cases. Of particular interest is the first ionization of PuO_2. We applied cutting-edge theoretical methods to refine the ionization energy, but our computed data fall in the range of ~6 eV and not in the ~7 eV region as the experiment dictates. Such a system requires further computational and experimental attention.

Introduction

In the last few decades the study of actinide chemistry in solid, solution, and gas phases has made great progress in fields including coordination chemistry,[1] molecular spectroscopy,[2,3] X-ray absorption spectroscopy,[4,5] laser ablation matrix isolation spectroscopy,[6,7] and environmental chemistry.[8,9]

Despite these advances, handling actinide materials poses significant hazards, such that laboratory studies and control of actinides in the environment remain major challenges. Many aspects of actinide chemistry are "exotic", which may largely be attributed to the participation of their 5f electrons in chemical bonds. Moreover, the fact that the 6d and the 7s shells are close in energy to the 5f shell raises problems in the determination of the ground and excited states of actinide molecules, and makes some types of experiments more challenging and the results uncertain. An example is the indeterminate population of low-lying metastable states, rather than the ground state, during electron impact (EI) studies, which can result in the erroneous determination of properties, such as ionization energies or dissociation energies of small linear triatomic AnO_2 [An = U, Pu] species.[10]

Theoretical chemistry can often guide experiments by predicting the outcome of reactions of actinides in the gas-phase and solution, and their spectroscopic and molecular properties. The predictive power of theory largely lies in how accurately it describes the relevant contributions of electronic effects in a molecule. For actinide elements, relativistic and correlation effects are paramount. In addition, the 5f, 6d, and 7s shells lie so close in energy that the probability of having a multideterminant ground state is very high and a proper description of the total energy needs to include accurately the electron correlation and the spin−orbit coupling (SOC). A simultaneous precise description of all these contributions remains a great challenge, and the computed molecular properties of actinide-containing species typically have larger inherent errors than is usually the case for lighter elements.

Given the special challenges posed by the actinides in both experiments and theory, it is clear that experiment and theory should be employed in a coordinated manner to most effectively and reliably evaluate the properties of actinide species. In recent years, such joint ventures have been proved to be effective, and in some cases very useful in disentangling some persistent problematic issues. Among the most notable cases was the assessment of the ground states of the CUO and UO_2 molecules, which were studied experimentally by laser-ablation matrix isolation spectroscopy.[7,11] The conundrum regarding the ground states of these molecules motivated theoreticians to evaluate with very high precision the electronic spectra of these molecules using several methods, which have all indistinguishably agreed on the determination of the ground state of UO_2[12−15] but have left some controversy in the case of the CUO molecule.[16,17] In contrast to theory elucidating experimental results, a remarkable feat was achieved when theory confidently predicted the ionization energy (IE) of UO_2 to be higher than the accepted experimentally determined value,[15] thus leaving experimentalists compelled to use a more precise technique to measure this parameter. The resulting definitive measurement using REMPI spectroscopy confirmed the theoretical prediction, which had been in contradiction with the previously accepted experimental value.[18,19]

* To whom correspondence should be addressed. E-mail: iinfant76@gmail.com (I. I.), gagliard@umn.edu (L. G.).
† Euskal Herriko Unibertsitatea and Donostia International Physics Center.
‡ Budapest University of Technology and Economics.
§ University of Geneva.
|| Lawrence Berkeley National Laboratory.
⊥ University of Minnesota and Supercomputing Institute.

10.1021/jp1016328
Published on Web 03/23/2010

This "pushing to the limit" the frontier of chemistry has also exposed the limitations of the various theoretical methods and experimental techniques, with several theory/experiment discrepancies having not yet been fully resolved. An example of a persistent discrepancy is the assessment of the IE for the PuO_2 molecule.[20−23] In a recent paper, we attempted to tackle this incongruity, by employing multiconfigurational wave functions followed by second-order perturbation theory, and spin−orbit coupling, the SO-CASPT2 method.[24] However, the computed IE, at 6.20 eV, is still considered too low as compared to the range established by the electron-transfer bracketing method, which is 7.03 ± 0.12 eV.[20] Despite that a theory/experiment difference still remains, our previous work was crucial to discount the previously measured IE using the EI technique, which gave a much higher value of 10.1 ± 0.1 eV.[10]

In a recent article, Marçalo and Gibson reviewed the gas-phase energetics of neutral, singly and doubly charged actinide dioxide and monoxide molecules.[25] They revised previous values of bond dissociation energies, ionization energies, and enthalpies of formation for the actinide series oxides from thorium up to curium. Despite this evaluation, it is clear that the experimental measurements for many of these molecules are not definitive, as reflected in the assigned uncertainties. In some cases, Marçalo and co-workers employed an electron-transfer bracketing method to obtain a range in which the IE resides. Specifically, they examined reactions of monopositive actinide molecules with species having very well assessed IEs. If during collision electron transfer occurs, then the IE of the actinide molecule is higher than that of the reference molecule; if charge transfer does not occur, the IE is lower. Such "bracketing" allows the assignment of an IE with an error bar somewhat larger than an error that would typically result if the IE were measured directly by a spectroscopic technique.[18] Although the uncertainties associated with the electron-transfer bracketing technique are generally somewhat large (e.g., ca. ±0.1 eV), it is a well established approach to reliably bracket first IEs. The most likely source of any systematic error in the bracketed range would result from excited-state molecular ions, which would give an apparent IE that is higher than the actual value. In the case of IE[PuO_2], for example, if the PuO_2^+ ions in the electron-transfer experiments were not effectively thermalized, the actual IE would be higher than the reported value of 7.03 ± 0.12 eV.[26]

In this work we investigate the trend of the first and second ionization energies of AnO_2 and AnO, for An = Th, Pa, U, Np, Pu, Am, and Cm, using the most accurate theoretical currently methods currently available. For the most controversial case, the IE of PuO_2,[24] we have improved upon existing results by employing one of the most recently developed techniques, the SO-RASPT2 approach.[27,28] Our goal is to address unambiguously where theory stands for these oxide species, and to identify areas for improvement in both theory and experiment.

Methods Section

First and second ionization energies, IE1 and IE2, of the AnO and AnO2 oxides were calculated in this work, corresponding to formation of the mono-cations and di-cations respectively. All calculations were performed using the complete active space (CAS) SCF method followed by multiconfigurational second-order perturbation theory (CASPT2).[29,30] Scalar relativistic effects were included using the Douglas−Kroll−Hess Hamiltonian and relativistic ANO-RCC basis set of VTZP quality,[31,32] as implemented in the MOLCAS 7.4 package.[33] Spin−Orbit coupling was included using the complete active space interaction method, CASSI,[34] which employs an effective one-electron spin−orbit (SO) Hamiltonian, based on the mean field approximation of the two electronic part.[35] This approach has been successful in studying many actinide-containing systems.[13,36−44]

In the CASSCF treatment, the ideal active space of AnO_2 [An = Th, Pa, U, Np, Pu, Am, and Cm] would be composed of 19 orbitals, 13 of which come from a linear combination of the 5f, 6d, and 7s orbitals of the actinide atom and the remaining 6 from the 2p orbitals of the oxygen atoms. This means that the smallest active space, the one for ThO_2, would contain at least 12 electrons, that is, 4 valence electrons from the Th and 8 valence electrons from the oxygen 2p orbitals. Unfortunately, an active space of (12e/19o) is computationally unfeasible due to the large amount of configuration state functions. We thus decided to truncate the space by removing the two lowest π_g bonding orbitals and the corresponding antibonding orbitals and one σ_g* antibonding orbital. This yields a more affordable space of (8e/14o). By applying the same truncation along the series, the largest active space, (14e/14o) is the one employed for CmO_2. For the actinide monoxides, the active space does not require any truncation. The ideal active space includes 16 orbitals, 13 from the actinide, and 3 from the oxygen. The largest active space is the one for CmO, (14e/16o). In the subsequent CASPT2 calculations, the orbitals up to the 5d of the actinide and the 1s of oxygen were kept frozen, while the remaining valence and semivalence orbitals, now including the 6s and 6p of the actinide and the 2s of oxygen, were correlated. The equilibrium geometries and harmonic frequencies for the ground and some of the excited states were determined by fitting fourth-order polynomials on discrete representations of the potential energy surfaces. As most of these molecules are known to be linear in their ground state, we have only considered the displacements along the symmetric stretch of the An-O bond for the AnO_2 species. The only exception is represented by ThO_2, which presents a bent geometry and was optimized using numerical gradients as implemented in MOLCAS.

Some of the calculations were performed using the recently developed RASPT2 method.[27] This approach differs from the CASPT2 method because it is based on a RASSCF reference wave function, rather than the CASSCF reference wave function. Unlike in CASSCF, in RASSCF the active space is divided in three different subspaces, called RAS1, RAS2, and RAS3. RAS1 and RAS3 can be considered extensions of the RAS2 space, where all the possible excitations can occur. RAS1 is the occupied space from which a limited number of electrons can be excited; RAS3 is the unoccupied space to which a limited number of electrons can be excited. RASSCF allows a larger flexibility in the choice of the active space, because it gives the possibility of choosing different type of excitations, whether they are SD (singles and doubles), SDT, SDTQ, and so on, between RAS1 and RAS3 depending on the type of system involved. Computing molecular properties only with the RASSCF method results in incomplete and possibly inaccurate results for mainly two reasons: (1) the size of the RAS space is usually too small to recover all the dynamic correlation effects; (2) the lack of size-extensivity. To improve upon these drawbacks, the RASPT2 method has been developed, in which second-order perturbation theory is included to retrieve the missing terms. The general notation for a RASPT2 calculation is (ae,ao)/(ae2,ao2)/max, where ae is the number of active electrons in RAS1 and RAS2 combined, ao is the number of active orbitals in all the RAS subspaces, ae2 is the number of active electrons in RAS2, ao2 is the number of active orbitals in RAS, max is the maximum number of excitations permitted out of RAS1 and into RAS3. To corroborate the CASPT2 results, we decided to

TABLE 1: First and Second Ionization Energies (eV) for the AnO_2 Series at Various Llevels of Theory[a]

	state	CASPT2	X2C-DC−CCSD	X2C-DC−CCSD(T)	SO-CASPT2	exp
			AnO_2			
Th	$^1A_1$	8.50	8.59	8.59	8.50	8.9 ± 0.4
Pa	$^2\Sigma_{0.5g}$	5.70	5.92	6.03	5.70	5.9 ± 0.2
U	$^3\Phi_{2u}$	6.20	6.01	6.03	6.21	6.128 ± 0.003
Np	$^4H_{3.5g}$	6.33	5.94	6.04	6.27	6.33 ± 0.18
Pu	$^5\Phi_{1u}$	6.43	5.82	5.93	6.20	7.03 ± 0.12
Am	$^6\Pi_{2.5u}$	6.71	6.57	6.46	6.76	7.23 ± 0.15
Cm	$^7\Sigma_{0g}$	8.39	7.85	7.68	8.27	8.5 ± 1.0
			AnO_2^+			
Th	$^2\Sigma_{0.5u}$	15.10	15.87	15.40	15.10	16.6 ± 1
Pa	$^1\Sigma_{0g}$	16.99	16.94	16.88	16.99	16.6 ± 0.4
U	$^2\Phi_{2.5u}$	14.51	14.26	14.14	14.36	14.6 ± 0.4
Np	$^3H_{4\,g}$	15.37	15.22	15.04	15.58	15.1 ± 0.4
Pu	$^4\Phi_{1.5u}$	15.48	15.94	15.72	15.37	15.1 ± 0.4
Am	$^5\Sigma_{0g}$	16.75	16.91	16.79	16.28	15.7 ± 0.6
Cm	$^6\Pi_{0.5g}$	15.97	15.90	15.75	16.15	17.9 ± 1.0

[a] The values for X2C-DC−CCSD and X2C-DC−CCSD(T) are computed at the spin free CASPT2 geometries. The cited experimental values are obtained through indirect measurements using the FTICR/MS method by Marçalo and Gibson.[25] The IE[AnO_2] for An = Np, Pu, and Am were obtained by electron-transfer bracketing; the IE[UO_2]value was accurately determined by Han et al.[18,19] using the REMPI method. The geometries have been optimized at SO-CASPT2 level of theory.

perform further calculations at different levels of theory. For this scope, we used the DIRAC08 program[45] (see http://dirac.chem.sdu.dk) that has some advantages that were beneficial for our objectives: (a) the inclusion of relativistic effects via a one-step exact (infinite order) 2-component relativistic Hamiltonian (X2C)[46] (b) the possibility of including the spin−orbit coupling term directly from the outset, however still with the possibility to perform an exact separation of the spin-free and spin-dependent terms of the Dirac−Coulomb (DC) Hamiltonian;[47] (c) the availability of computing electron correlation with the most accurate single-reference methods such as X2C-DC−CCSD and X2C-DC−CCSD(T).[48,49] In the 4-component framework, the two-electron interaction is generally described by a simple Coulombic term plus a retardation effect called Breit interaction. This latter contribution is usually very small for chemical purposes and is normally neglected. The two-electron interaction used includes only the Coulomb term, hence the acronym DC, which stands for Dirac-Coulomb. In all these CC calculations, the computed correlation energy depends on the correlated electrons. We correlated the electrons residing in the 6s, 6p, 5f, 6d, and 7s orbitals of the actinide atom in addition to the 4 valence electrons of the 2p orbitals of the oxygens. We then restricted the set of virtual orbitals to those relevant to valence and subvalence correlation. We did so by deleting virtual orbitals with an orbital energy above 10 au. In the CC calculations, the Dyall uncontracted double-ζ basis for the actinide atoms of 26s23p17d13f2g size was used.[50] This basis set has been shown to perform well for small triatomic actinide dioxide molecules.[51] For the lighter oxygen element we made use of a cc-pVDZ and cc-pVTZ basis sets by Dunning.[52]

Results

The computed and experimental first and second IEs of the AnO_2 and AnO are summarized in Tables 1 and 2, respectively. The ground state orbital compositions of the $AnO_2^{[0,+,2+]}$ and $AnO^{[0,+,2+]}$ are summarized in Tables 3 and 4, respectively. Specific aspects of the computational results are discussed below.

TABLE 2: First and Second Ionization Energies (eV) for the AnO Series[a]

	state	CASPT2	X2C-DC−CCSD	X2C-DC−CCSD(T)	SO-CASPT2	exp
			AnO			
Th	$^1\Sigma_0$	6.58	6.41	6.55	6.56	6.6035 ± 0.0008
Pa	$^2\Phi_{2.5}$	6.48	6.38	6.51	6.28	5.9 ± 0.2
U	$^5I_4$	6.04	5.91	5.98	6.05	6.0313 ± 0.0006
Np	$^6\Phi_{3.5}$	5.98	5.98	6.05	5.97	6.1 ± 0.2
Pu	$^7\Pi_0$	6.16	5.94	5.99	6.17	6.1 ± 0.2
Am	$^8\Sigma_{0.5}$	6.24	6.04	6.06	6.21	6.2 ± 0.2
Cm	$^9\Sigma_0$	6.68	6.42	6.46	6.68	6.4 ± 0.2
			AnO^+			
Th	$^2\Sigma_{0.5}$	11.94	11.92	11.99	11.94	11.8 ± 0.7
Pa	$^3H_4$	11.91	12.17	12.27	12.10	11.8 ± 0.7
U	$^4I_{4.5}$	12.99	12.32	12.30	13.07	12.4 ± 0.6
Np	$^5\Phi_4$	13.50	13.34	13.29	13.43	14.0 ± 0.6
Pu	$^6\Pi_{0.5}$	14.56	14.31	14.20	14.36	14.0 ± 0.6
Am	$^7\Sigma_0$	15.12	15.91	15.79	15.05	14.0 ± 0.6
Cm	$^8\Sigma_{0.5}$	15.99	15.24	15.21	15.92	15.8 ± 0.4

[a] The values for X2C-DC−CCSD and X2C-DC−CCSD(T) are computed at the spin free CASPT2 geometries. Most of the experimental values were obtained through indirect measurements as described in the assessment by Marçalo and Gibson;[25] IE[ThO] and IE[UO] were accurately measured by Heaven and co-workers using the REMPI method 0.[3,18,19,55,58] The geometries have been optimized at SO-CASPT2 level of theory.

TABLE 3: Orbital Composition for the Spin-Free Ground State (GS) of the AnO_2, AnO_2^+, and AnO_2^{2+} Systems Computed at CASSCF/CASPT2 Level of Theory[a]

	state	composition	Å
		AnO_2	
Th	$^1A_1$	67% $(\sigma_u[\text{bonding}])^2$	1.923 (bent)
Pa	$^2\Sigma_{0.5g}$	96% $(7s)^1$	1.816
U	$^3\Phi_{2u}$	90% $(7s)^1(5f\phi)^1$	1.827
Np	$^4H_{3.5g}$	92% $(7s)^1(5f\delta)^1(5f\phi)^1$	1.761
Pu	$^5\Phi_{1u}$	96% $(7s)^1(5f\delta)^2(5f\phi)^1$	1.744
Am	$^6\Pi_{2.5u}$	90% $(5f\pi)^1(5f\delta)^2(5f\phi)^2$	1.807
Cm	$^7\Sigma_{0g}$	87% $(5f\pi)^2(5f\delta)^2(5f\phi)^2$	1.832
		AnO_2^+	
Th	$^2\Sigma_{0.5u}$	92% $(\sigma_u[\text{bonding}])^1$	1.832
Pa	$^1\Sigma_{0g}$	94% $(\sigma_u[\text{bonding}])^2$	1.767
U	$^2\Phi_{2.5u}$	98% $(5f\phi)^1$	1.745
Np	$^3H_{4g}$	93% $(5f\delta)^1(5f\phi)^1$	1.723
Pu	$^4\Phi_{1.5u}$	93% $(5f\delta)^2(5f\phi)^1$	1.704
Am	$^5\Sigma_{0g}$	85% $(5f\delta)^2(5f\phi)^2$	1.721
Cm	$^6\Pi_{0.5g}$	84% $(5f\pi)^1(5f\delta)^2(5f\phi)^2$	1.746
		AnO_2^{2+}	
Th	$^1\Sigma_{0g}$	77% $(\sigma_u[\text{bonding}])^0$	1.903
Pa	$^2\Sigma_{0.5g}$	93% $(\sigma_u[\text{bonding}])^1$	1.726
U	$^1\Sigma_{0g}$	92% $(\sigma_u[\text{bonding}])^2$	1.710
Np	$^2\Phi_{2.5u}$	92% $(5f\phi)^1$	1.700
Pu	$^3H_{4g}$	98% $(5f\delta)^1(5f\phi)^1$	1.675
Am	$^4\Phi_{1.5u}$	88% $(5f\delta)^2(5f\phi)^1$	1.679
Cm	$^5\Sigma_{0g}$	85% $(5f\delta)^2(5f\phi)^2$	1.674

[a] The $(\sigma_u[\text{bonding}])^x$ with $x = 0,1,2$ refers to an orbital formed by the bonding combination between the $2p_z$ orbital localized on the oxygen atoms and the $5f\sigma_u$. This orbital is usually doubly occupied in all the species, with the exception of ThO_2, ThO_2^{2+}, and PaO_2^+. In these cases, the depletion of this orbital brings to an elongation of the An−O bond distance. Bond distances in Å are also given. The geometries have been optimized at SO-CASPT2 level of theory.

ThO_2 and ThO. The thorium atom has a $(6d)^2(7s)^2$, $^3F_2$, electronic ground state [http://www.lac.u-psud.fr/Database/Contents.html]. In ThO_2, the oxygen atoms withdraw charge from the metal, leaving the thorium atom with a formal charge of Th(IV) and an electronic configuration of $(6d)^0(7s)^0$. In this

TABLE 4: Orbital Composition for the Ground State (GS) of the AnO$^{[0,+,2+]}$ Molecules Computed at Spin-Free CASSCF/CASPT2 Level of Theory[a]

	State	Composition	Å
		AnO	
Th	$^1\Sigma_0$	88% $(7s)^2$	1.863 (1.840)[55]
Pa	$^2\Phi_{2.5}$	94% $(7s)^2(5f\phi)^1$	1.818
U	$^5I_4$	94% $(7s)^1(5f\delta)^1(5f\phi)^1(5f\pi)^1$	1.838 (1.8383(6))[19]
Np	$^6\Delta_{1.5}$	50% $(7s)^1(5f\delta)^2(5f\phi)^1(5f\pi)^1$ + 40% $(7s)^1(5f\delta)^1(5f\phi)^1(5f\pi)^1(5f\sigma)^1$	1.839
Pu	$^7\Pi_0$	78% $(7s)^1(5f\delta)^2(5f\phi)^2(5f\pi)^1$ + 15% $(7s)^1(5f\delta)^1(5f\phi)^2(5f\pi)^1(5f\sigma)^1$	1.820
Am	$^8\Sigma_{0.5}$	94% $(7s)^1(5f\delta)^2(5f\phi)^2(5f\pi)^2$	1.801
Cm	$^9\Sigma$	94% $(7s)^1(5f\sigma)^1(5f\delta)^2(5f\phi)^2(5f\pi)^2$	1.836
		AnO^+	
Th	$^2\Sigma_{0.5}$	93% $(7s)1$	1.827 (1.807)[55]
Pa	$^3H_4$	94% $(6d\delta)^1(5f\phi)^1$	1.804
U	$^4I_{4.5}$	94% $(5f\delta)^1(5f\phi)^1(5f\pi)^1$	1.796 (1.801(5))[56]
Np	$^5\Gamma_2$	28% $(5f\delta)^2(5f\phi)^1(5f\pi)^1$ + 22% $(5f\delta)^1(5f\phi)^1(5f\pi)^1(5f\sigma)^1$ + 20% $(5f\delta)^2(5f\phi)^2$	1.798
Pu	$^6\Pi_{0.5}$	79% $(5f\delta)^2(5f\phi)^2(5f\pi)^1$ + 14% $(5f\delta)^1(5f\phi)^2(5f\pi)^1(5f\sigma)^1$	1.789
Am	$^7\Sigma_0$	92% $(5f\delta)^2(5f\phi)^2(5f\pi)^2$	1.782
Cm	$^8\Sigma_{0.5}$	94% $(5f\sigma)^1(5f\delta)^2(5f\phi)^2(5f\pi)^2$	1.792
		AnO^{2+}	
Th	$^1\Sigma_0$	95% $(\sigma_u[\text{bonding}])^2$	1.790
Pa	$^2\Phi_{2.5}$	94% $(5f\phi)^1$	1.733
U	$^3H_4$	94% $(5f\delta)^1(5f\phi)^1$	1.720
Np	$^4I_{4.5}$	48% $(5f\delta)^1(5f\phi)^1(5f\pi)^1$ + 46% $(5f\phi)^1(5f\pi)^1(5f\sigma)^1$	1.723
Pu	$^5\Gamma_2$	70% $(5f\delta)^2(5f\phi)^1(5f\pi)^1$ + 20% $(5f\delta)^1(5f\phi)^1(5f\pi)^1(5f\sigma)^1$	1.731
Am	$^6\Pi_{0.5}$	75% $(5f\delta)^2(5f\phi)^2(5f\pi)^1$	1.808
Cm	$^7\Sigma_0$	66% $(5f\delta)^2(5f\phi)^2(5f\pi)^2$	1.791

[a] Bond distances in Å are also given. The geometries have been optimized at SO-CASPT2 level of theory. (Experimental bond distances are reported in parentheses.)

approximate picture, the bond would be purely ionic. However, it has been shown[53,54] that the 6d orbitals participate actively in the bond. The first excited level of Th with a 5f orbital contribution, $(5f)^1(6d)^1(7s)$,[2] $^3H_4$, lies about 1 eV above the $^3F_2$ ground state, meaning that the 5f orbitals lie relatively high in energy. For this reason in ThO_2 the bond between Th and O occurs mainly through the $6d\pi$(Th)−$2p\pi$(O) or $6d\sigma$(Th)−$2p\sigma$(O) interaction, with only little contribution from the $5f\sigma$ and $5f\pi$. This is confirmed by CASSCF calculations, which predict the correct mixture of Th 6d, 7s, 5f orbital in ThO_2. The total population on the $5f\pi$ is of only 0.3e versus the 1.0e of the $6d\pi$. This larger occupation of the 6d over the 5f, as explained extensively elsewhere,[53,54] supports the bending of the ThO_2. The first ionization energy (IE1) involves the removal of one electron from a moderately strong σ-bond, hence the computed value of 8.50 eV is much higher than the first IE of the remaining AnO_2, in which the electron is usually removed from a nonbonding orbital. The CASPT2 IE of ThO_2, Table 1, falls within the experimental range and has a negligible SO contribution, less than 0.01 eV. The coupled cluster values are also in good agreement with experiment. Computed values for IE2 with all methods are in general lower than the experimental value, which, however, has a large error bar.

In ThO, thorium has a formal charge of Th(II). The ground state of Th(II) is $(5f)^1(6d)^1$, $^3H_4$, with the $(6d)^2$, $(6d)^1(7s)^1$, and $(7s)^2$ levels lying 0.01, 0.68, and 1.48 eV, respectively, above the ground state. It is not unlikely that one of these states may become the ground state in ThO. In our calculations we find that the two nonbonding electrons belong to the 7s shell (Table 4). The ground state is then a closed shell, $^1\Sigma_0$. Goncharov and Heaven[55] have accurately measured the IE of ThO using pulsed field ionization-zero-kinetic-energy photoelectron spectroscopy (PFI-ZEKE) and provided an accurate value of 6.6035 ± 0.0008 eV. Our SO-CASPT2 calculation predicts a value of 6.56 eV, which should be compared with the multi reference configuration interaction (MRCI) value of 6.49 eV reported by Pitzer et al.[55] The spin-free X2C-DC-CCSD(T) method yields a value of 6.55 eV, similar to the CASPT2 value. This agreement among several approaches is due to the fact that the ground state of ThO is mainly single configurational. Furthermore, the first and second ionizations of ThO involve the depletion of the 7s shell, with a minor SO contribution, about 0.02 eV. All methods reproduce well the value of IE2.

PaO_2 and PaO. Protactinium is the first actinide with the 5f shell partially occupied in its ground state, $^4K_{11/2}$, $(5f)^2(6d)^1(7s)^2$. This suggests that the bonding pattern between Pa and the two oxygens in PaO_2 is different than that in ThO_2. The monocation, PaO_2^+, isoelectronic with ThO_2, is not bent, but linear, due to a more effective participation of the 5f orbitals in the bonding with the 2p of the oxygen atoms. In other terms, this is a three-center interaction facilitated by the 5f orbitals in the middle atom pushing the molecule toward a linear arrangement. The Mulliken population is 0.66e in the $5f\pi$ orbital and 0.90e in the $6d\pi$ orbital. As in ThO_2, also in PaO_2 the metal has a formal charge of 4+. This leaves only one unpaired nonbonding electron, belonging to the 7s shell, see Table 3. The ground state is represented by a single electronic configuration. The computed first IE with CASPT2 is 5.70 eV, which again falls in the bottom side of the estimated range, 5.90 ± 0.2 eV.[25] The X2C-DC-CCSD(T) method predicts a slightly larger value, 6.03 eV. SO coupling has little effect. The second ionization, IE2, compares well with the experiment for all the theoretical methods (Table 1).

In PaO, Pa has a formal charge of +2, leaving three nonbonding electrons that recombine in a doublet ground state, $(7s)^2(5f\phi)^1$, $^2\Phi_{2.5}$. The computed IE at spin-free CASPT2 level of theory, 6.48 eV, is greater than the previously estimated value, 5.90 ± 0.2 eV. In this case the SO coupling effect on IE is large and, with its inclusion, the estimated IE becomes 6.28 eV, closer to the previously estimated value. Such a large SO coupling can be understood by inspection of the electronic configuration of PaO^+, $(6d\delta)^1(5f\phi)^1$, $^3H_4$. Upon ionization an electron is removed from a 7s orbital, and one electron is promoted to the $6d\delta$ orbital. This latter orbital has a larger orbital angular momentum compared to the 7s and combines with the $5f\phi$ to give a total angular momentum of $\Omega = 4$. This explains the strong SO contribution. The X2C-DC-CCSD(T) IE value, 6.38 eV, is similar to the spin-free CASPT2 value. The same occurs for IE2, for which both theoretical methods compare well with experiment.

UO_2 and UO. The UO_2 molecule has been studied extensively. Historically, two triplet states have been considered good candidates to be the ground state, the $(7s)^1(5f\phi)^1$, $^3\Phi_{2u}$, and the $(5f\phi)^1(5f\delta)^1$, $^3H_{4\ g}$ states.[7] The latest theoretical results[12] agree with the REMPI experiment by Han et al.,[18] according to which the $^3\Phi_{2u}$ state is the ground state. Theoretical predictions of the first and second IE at different level of theories have provided very accurate values.[12−14]

The UO molecule has a $(7s)^1(5f\delta)^1(5f\phi)^1(5f\pi)^1$, $^4I_{4.5}$, ground state. Inspection of Table 4 shows that, according to our calculation, the dominating configuration, $5f^37s^1$, has a weight of 94%. This result is in slight discrepancy with the experimental

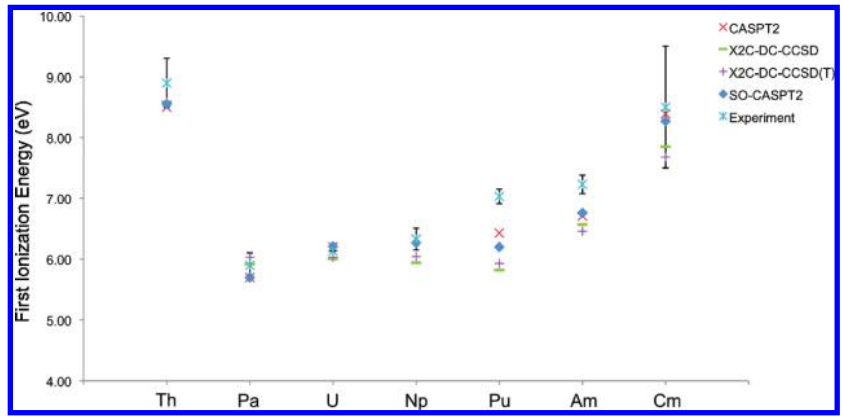

Figure 1. First ionization energies (eV), IE1, for the AnO_2 series computed at different level of theories. The experimental error bars are also shown for comparison.

results obtained by Heaven et at,[56] according to which the ground state of UO has leading eigenvector components that are 85% $5f^37s^1$ and 15%$5f^27s^2$. Upon ionization the electron is removed from a 7s shell, and as a consequence the SO effect on IE1 is only about 0.01 eV. This molecule was studied at the CASPT2 level of theory by Paulovic et al.,[57] who reported a IE1 value of 6.05 eV, in agreement with the experimental value measured by Goncharov et al.,[58] 6.0313 ± 0.0006 eV. Paulovic et al.[57] did not report a value for IE2, which we now report in this study. With our active space choice, we obtained an IE1of 6.06 eV, differing only by 0.01 eV from the value reported in ref 57. We also obtained an IE2 value of 12.99 eV at the spin-free level and 13.07 eV including SO coupling. Both values fall on the upper limit of the experimental error bar, 12.4 ± 0.6 eV. Spin-free X2C-DC−CCSD(T) predicts a value of 12.30 eV.

NpO_2 and NpO. Although the ground and excited states of the NpO_2^+ and NpO_2^{2+} have been already studied,[51,59−61] to our knowledge this is the first study on the neutral dioxide. The ground state of NpO_2, $^4H_{3.5g}$, is mainly composed by a single electronic configuration $(7s)^1(5f\delta)^1(5f\phi)^1$. Upon ionization, the molecule looses a 7s electron; therefore also in this case the SO effect on IE1 is only about 0.07 eV. The IE1 value computed including SO coupling, 6.27 eV, is close to the experimental value determined by Gibson et al. using the electron-transfer method, 6.33 ± 0.18 eV.[23] The spin-free X2C-DC−CCSD(T) provides a slightly smaller value of 6.04 eV. The second ionization IE2 involves the removal of a 5fδ electron, hence changing the total angular momentum Ω from 4_g in NpO_2^+ to 2.5_u in NpO_2^{2+}. The smaller coupling in the dication determines an enlargement of the gap, as compared to the spin-free case, in favor of the monocation by a significant amount, 0.21 eV. The SO-CASPT2 value for IP2,15.58 eV, is slightly larger than the experimental value, 15.1 ± 0.4 eV.[23] On the other hand, the spin-free X2C-DC-CCSD(T) value for IE2 is 15.04 eV, and adding the 0.21 eV SO contribution, it fits well inside the experimental range.

The NpO diatomic presents a multiconfigurational ground state, $^6\Phi_{3.5}$, composed of 50% $(7s)^1(5f\delta)^2(5f\phi)^1(5f\pi)^1$ and 40% $(7s)^1(5f\delta)^1(5f\phi)^1(5f\pi)^1(5f\sigma)^1$. The eye-catching feature is that this is the first molecule that presents a multireference character among all the species analyzed so far. Among all the molecules examined, this feature occurs only for NpO and PuO and their respective mono- and dications, while the other have mainly a single-reference character. As in the other monoxides, the first ionization involves the removal of one electron from the 7s orbital. The CASPT2 value for IP1 is 5.98 eV and the X2C-DC−CCSD(T) value is 6.05 eV. Spin−orbit coupling effect is about 0.01 eV.

PuO_2 and PuO. The first ionization energy IE1 of PuO_2 has recently been the subject of several theoretical and experimental investigations. Early studies using electron impact ionization threshold measurements provided values of IE1 ranging from 9.4 ± 0.5 eV[62] to 10.1 ± 0.1 eV.[10] Santos et al.,[20] a few years later, employed electron transfer bracketing and determined a new value of 7.03 ± 0.12 eV, more in line with the first ionization energies of UO_2, 6.128 ± 0.003 eV[18] and NpO_2, 6.33 ± 0.18 eV;[23] such an increase in IE[AnO_2] across the series from UO_2 to PuO_2 is as expected.[25] Subsequently, a new EI measurement gave a value for IE1 of 6.6 eV.[63] To establish with more certainty which of the above experimental values is more accurate, we performed a CASPT2 study of PuO and PuO_2.[24] Our best estimate for IE1 of PuO_2 was 6.20 eV with the inclusion of the SO effects. Although this value is in reasonable agreement with the Santos et al. experiment,[20] it is about 0.7 eV below the left side of their experimental error bar. Inspection of Table 1 and Figure 1 shows that this is the largest discrepancy between theory and experiment for IE1 for all of the species examined. To better understand this incongruity, we have performed new calculations on PuO and PuO_2. We already pointed out in the methodological section that when we chose the active space in the CASSCF calculation for all the dioxides, we had to omit two of the occupied bonding π_g orbitals. Such a truncation may introduce large errors in the evaluation of the ionization energy in certain cases. We have thus performed some RASPT2 calculations.

The PuO_2 molecule presents a single configurational, $(7s)^1(5f\delta)^2(5f\phi)^1$, $^5\Phi_{1u}$, ground state. Starting from our old results from a CASSCF/CASPT2 calculation with 12 electrons in 14 orbitals, we decided to carry out a RASSCF/RASPT2 calculation correlating the same total number of electrons and orbitals, but using a RASSCF reference wave function different from the prior CASSCF wave function. We denote it as (12/14)/(4,5)/2: we included in RAS2 the orbitals that form the open-shell configuration, namely 7s, 5fδ^+, 5fδ^-, 5fϕ^+, and 5fϕ^-, and we employed only singles and doubles excitations from RAS1 and to RAS3, which have been sufficient to describe accurately the IE of highly conjugated systems.[28] More specifically, in RAS1 we included the σ_g and π_u bonding molecular orbitals between oxygen and plutonium. The newly computed IE1 is 6.32 eV, 0.11 eV smaller than the CASPT2 value, 6.43 eV, reported in Table 1. This is already a good agreement, since it falls within the maximum error of the CASPT2 method, which is considered to be around 0.2 eV.[41] We decided to improve the results by including the two bonding π_g orbitals in RAS1 and, in RAS3, the unoccupied antibonding π_u* and the σ_g*, which were not included in the CASSCF/CASPT2 calculations. This more

balanced active space, denoted as (16/19)/(4,5)/2 predicts a value of 6.09 eV, which is in even worse agreement with the experimental value of Santos et al.[20] We repeated the calculations with up to quadruple excitations, denoted as (16/19)/(4/5)/4 and we obtained a value of 6.08 eV, very close to the one computed using only singles and doubles excitations. All these values are close to the X2C-DC-CCSD(T) value, 5.93 eV, which may be considered very accurate due to the single-reference character of the ground state of both neutral and monocationic PuO_2. We consider these last results definitive from the computational point of view, and we now confirm that the first ionization of PuO_2, at least from a computational standpoint, is closer to 6 eV rather than 7 eV.

We do not see how the theoretical results could be much improved at this time, since we are already using cutting-edge theoretical approaches, which have been proved in the past to be very accurate. Using even larger basis sets and/or active space would have only a minor effect at this point. It would certainly be worthwhile to perform an experiment in which a direct and accurate spectroscopic measurement of the IE of the PuO_2 molecule is performed, in analogy to what was done for the UO_2 molecule by Han et al.;[18] however, due to the much greater hazards in handling plutonium as compared with uranium, such experiments are currently impractical and the electron-transfer value for IE[PuO_2], 7.03 ± 0.12 eV, is currently considered the most reliable experimental value.

We also computed the IE2 at RASPT2 level of theory, using a larger active space, (16/19)/(4/5)/4. We obtained a value of 15.07 eV, about 0.4 eV smaller than the one resulted from the (12/14) space. This new value falls well inside the experimental error bar, 15.1 ± 0.4 eV.

AmO_2 and AmO. Americium has a $(5f)^7(6d)^0(7s)^2$ ground state. We previously studied Am mono- and dioxide and determined spectroscopic properties for the ground state and several excited states.[64] In AmO_2, corresponding to formal Am(IV), the two 7s and two 5f electrons are withdrawn by the oxygen atoms, and the ground state of the molecule is a sextet state,$^6\Pi_{2.5u}$, $(5f\pi)^1(5f\delta)^2(5f\phi)^2$. This is the first actinide dioxide along the series in which the 7s shell is empty and only the 5f shell is occupied. The increase of the nuclear charge along the series amplifies the screening effect of the 5f electrons and as a result the 5f shell is more stabilized than the 7s. As a consequence, the 5f electrons participate less in the bond, with subsequent increase of the Am−O bond distance as compared to the earlier actinides (see Table 3), despite a diminished ionic radius size along the series. This trend is confirmed by the contribution of only 0.18e to the bond of the 5f orbitals according to Mulliken population analysis. Upon ionization, the electron is detached from a core-like 5f orbital, and the energy required to remove it is higher than that needed to remove a 7s electron. The computed IE1 at SO-CASPT2 level of theory is 6.76 eV, about 0.5 eV larger than the computed IE1 of PuO_2, NpO_2 and UO_2. The same trend is confirmed for IE2, for which the SO-CASPT2 value is 16.28 eV, almost 1 eV higher than the earlier species. Recently, Notter et al.[65] computed the ground and excited states of the AmO_2^{n+} [n = 1, 2, 3] cations at 4c-DC−CCSD level of theory, but they did not report ionization energies. We thus performed spin-free X2C-DC-CCSD(T) calculations, which gave a smaller IE1, 6.46 eV (vs the 6.71 of the SF-CASPT2) and a somewhat similar IE2, 16.79 eV (vs 16.75 eV, SF-CASPT2). Although the CCSD(T) IE1 value is smaller than the CASPT2 value, it is about 0.4 eV larger than for NpO_2, PuO_2, and UO_2. One should also notice the reduction of IE2 by almost 0.5 eV upon inclusion of SO coupling. This can be understood by inspecting the Ω values. For the monocation it is equal to zero, hence SO coupling will be minor. On the other hand, the Ω value for the dication, equal to 1.5 and gives a large SO recombination and as a consequence a large value for IE2.

In the mono-oxide, americium has a formal oxidation state Am(II). Seven unpaired electrons contribute to the octet ground state, $^8\Sigma_{0.5}$, $(7s)^1(5f\delta)^2(5f\phi)^2(5f\pi)^2$. Unlike in AmO_2, one electron occupying the 7s orbital is removed upon ionization. The IE1 is similar to the others actinide mono-oxides, 6.21 eV at SO-CASPT2 level of theory. This is in agreement with the experimental value, 6.2 ± 0.2 eV, which is also similar to the IE1 of the other AnO. In our previous study, in which we used a different active space we also obtained a value of 6.2 eV.[64] Also in this case SO coupling has a minor contribution to IE1, about 0.03 eV. The second electron to be removed is a 5f electron and the computed value of IE2 is 15.05 eV, much larger than for the other actinide mono-oxides. All theoretical methods confirm this trend for the values of IE2 along the monoxide series, as illustrated in Table 2. On the other hand, experiment presents wide error bars and no obvious trend.

CmO_2 and CmO. The ground state of CmO_2 is the $^7\Sigma_{0\ g}$ septet state, mainly composed by the $(5f\pi)^2(5f\delta)^2(5f\phi)^2$ electronic configuration.[64] As in AmO_2, all the unpaired electrons occupy the 5f shell. The core-like feature is more pronounced, and IE1 is equal to 8.27 eV at SO-CASPT2 level of theory, a value significantly larger than the previous ones. There is no experimental value for IE1; however, the value has been estimated as 8.5 ± 1 eV,[25] in agreement with the computed values. The SO-CASPT2 method predicts the IE2 within the experimental error bar, while the CC results fall below it.

In CmO the ground state is a nonet $^9\Sigma_0$ state composed mainly by $(7s)^1(5f\sigma)^1(5f\delta)^2(5f\phi)^2(5f\pi)^2$. The first electron is removed from the 7s orbital and it corresponds to a IE1 value about 0.4 eV higher than for the other actinide monoxides. Experiment shows a wide error bar for IE2, 15.8 ± 0.4 eV. All our methods consistently give a value of ca. 16 eV.

Discussion

We will now present a discussion of the trends of the ionization energies for the species examined. The computed and experimental ionization energies for the AnO_2, AnO_2^+, AnO, and AnO^+ are plotted in Figures 1−4.

In AnO_2, as previously mentioned, An has a formal oxidation state of IV and in AnO of II. This does not mean that the electronic configuration of the oxides will be directly comparable to the corresponding atomic ions because oxygen interacts with the 5f, 6d, and 7s shells and changes the atomic energy levels. It is, however, frequently the case that the open-shell electrons are localized on the actinide center and an atomic-like interpretation can be useful.

The IE trends along the actinide series depends on the balance between three primary factors: (a) the nuclear charge increase makes the outer electrons more bound and hence less susceptible to ionization; (b) the increase of electron repulsion makes the mono- and dioxides more prone to be ionized; (c) the different relative stabilization of the 5f and 7s shells, and in some cases the 6d shell, determines a different orbital occupation along the series.

Let us begin with the actinide dioxides. ThO_2 represents a distinctive case because the first electron to be ionized belongs to a σ-bonding orbital, hence IE1 is large compared to the other dioxides. From PaO_2 to CmO_2, two types of orbitals can be occupied, the 7s and the 5f (see Table 3 for details on the orbital

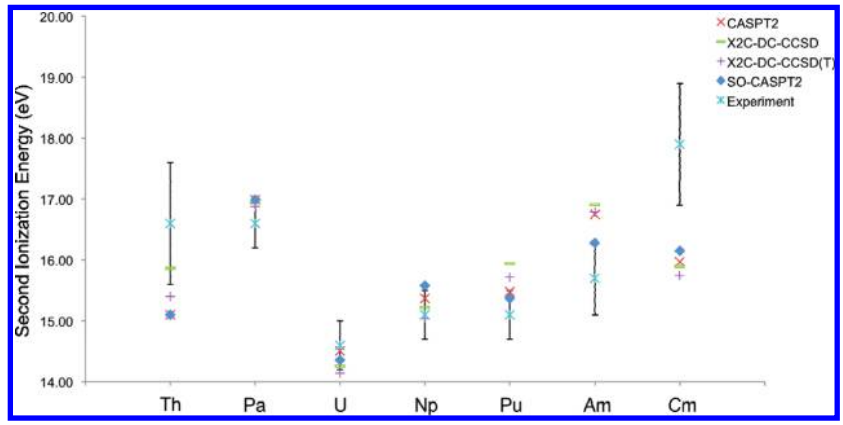

Figure 2. Second ionization energies (eV), IE2, for the AnO_2 series computed at different level of theories. The experimental error bars are also shown for comparison.

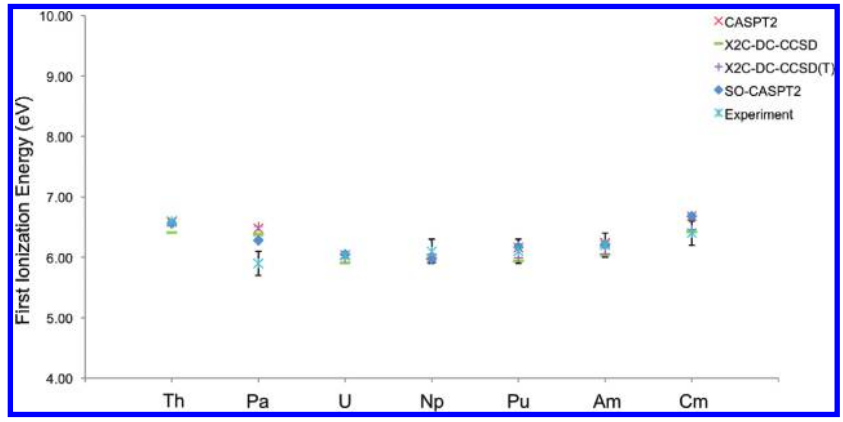

Figure 3. First ionization energies (eV), IE1, for the AnO series computed at different level of theories. The experimental error bars are also shown for comparison.

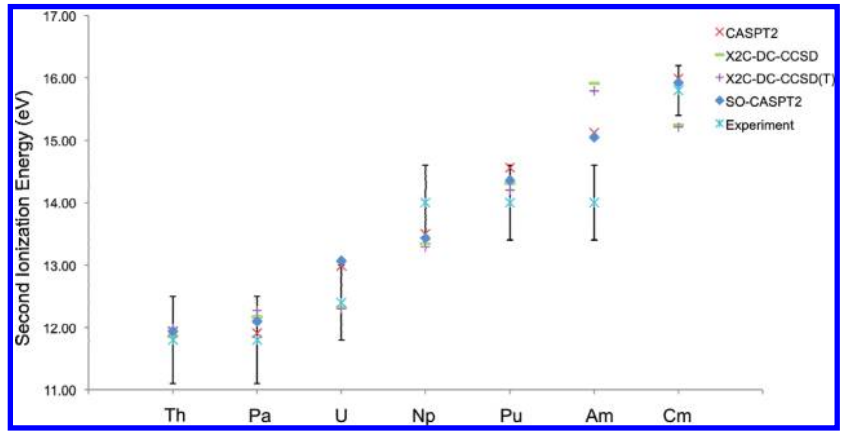

Figure 4. Second ionization energies (eV), IE2, for the AnO series computed at different level of theories. The experimental error bars are also shown for comparison.

occupation). For the early PaO_2 molecule, the core electrons of Pa screen both the 7s and the 5f electrons; however, the 7s orbital has a larger penetration than the 5f orbital, hence it is occupied first. Upon adding electrons, the 5f shell also becomes partially occupied and the following effects occur: the effective nuclear charge increases along the series and the 7s orbital becomes more bound but, at the same time, the 5f shell is better stabilized compared to the 7s shell, due to a better penetration of the former in the core region with increasing electron density. This last feature allows the occupation of the 7s shell up to PuO_2, whereas for AmO_2 and CmO_2 only the 5f orbitals are occupied. The electronic configurations of the cations are easier to interpret. The large increase of the nuclear effective charge contracts the orbital space of the valence electrons such that the 5f orbitals penetrate the core region better than the 7s orbitals and their energy drops below the energy of the 7s orbital. When the neutral species has one 7s electron, this will be the first electron to be ionized.

As already stated, the larger penetration of the 7s orbital in the core region upon adding electrons in the 5f shell (i.e., moving from left to right along the actinide series), increases the ionization energy. This trend is reproduced in our calculations at the spin-free CASPT2 level of theory (see Table 1), with a smooth increase of IE1 from PaO_2 to PuO_2. The addition of the SO coupling modifies this trend because the interaction between the spin motion and the orbital motion is of the same order of magnitude as the stabilization of the 7s along the series and the two effects may either cancel out or add up. As is evident in

Figure 1, the experimental values for IE1 suggest a continuous increase between PaO_2 and AmO_2, as would be expected based on the increase in the nuclear charge. In contrast, the computed value for PuO_2 in particular suggests that the SO coupling effect there breaks that expected trend. As remarked above, although there is no reason to doubt the experimental IE[PuO_2] reported by Santos et al.,[20] it would be worthwhile, albeit very challenging, to confirm and refine this value spectroscopically, and thereby definitively evaluate whether the remarkable computed deviation for PuO_2 in the trend of IE1 across the AnO_2 series is valid. For AmO_2 and CmO_2, IE1 is higher because the ionization involves the more core-like 5f electrons. CmO_2 presents the largest IE1 because the neutral molecule has a stable half-filled 5f shell configuration. This trend is also confirmed by the experimental measurements.

The second ionization of AnO_2, for An = U, Np, Am, and Cm, involves the removal of a 5f electron. As a consequence of the stabilization that occurs for the 5f shell across the series, IE2 also increases along the series, as confirmed by the calculations. For ThO_2 and PaO_2, the IE2 correspond to removal of an electron from a σ-bonding orbital; hence these IE2 are higher than for the other dioxides. The experimental IE2 also reveal the same general trend across the series.

We discuss now the IE's trend for the actinide monoxides. Across the series, from ThO to CmO, a 7s electron is always removed upon first ionization. This would imply that IE1 smoothly increases across the series; however this is not the case, according to the spin-free calculations (Table 2). The first two molecules, ThO and PaO, present a larger IE1 compared to the others (with the exception of CmO), but this can be attributed to the removal of an electron from a stable $7s^2$ closed shell. In PaO the situation is further complicated by the fact that the ionized molecule shows a more favorable penetration of the 6d in the core region, rather than the 7s, hence implying the occupation of a 6d and a 5f orbital. From UO to NpO, the trend is clear, although not perfect from a computational standpoint. The minimum of IE1 is reached for NpO at spin-free CASPT2 level of theory, or for UO and PuO at X2C-DC-CCSD(T) level of theory. The differences in IE1 among these species are well within the error of the computational methods. Moreover, NpO and PuO present a multiconfigurational ground state and a simple qualitative picture does not necessarily work. Experimentally, indeed the trend seems to be smoother; however, all of the measurements/estimates include rather large error bars. We must emphasize that for the neutral molecule, as stated above, the balance among several factors having opposite effects is crucial, especially for the elements in the middle of the series, U, Np, and Pu. For AmO, and especially for CmO, IE1 is relatively large. In the latter case, the 5f shell is high-spin "half-filled" plus the 7s with the same spin orientation. This evidently results in a further stabilization of the neutral molecule and a larger IE.

The trend of the AnO^+ species is easier to understand. As in the AnO_2^+ case, the ionization occurs from a 5f orbital, except for ThO (from 7s) and PaO (from 6d). Thus the augmented stabilization of the 5f electrons from U to Cm makes their IE2 values steadily increase across the series. This effect is also clearly revealed by the experimental values.

Conclusions

We presented the results of a computational study on actinide monoxides (AnO) and dioxides (AnO_2) for An = Th, Pa, U, Np, Pu, Am, and Cm. First and second ionization energies have been determined and compared with experimental values, when available. The trends along the series have been analyzed in terms of the electronic configurations of the various species. The agreement with experiment is excellent in most cases; however, the IE1 of PuO_2 remains an unresolved conundrum deserving further computational and experimental attention with advanced methodologies in future work.

Acknowledgment. This work was supported by the Director, Office of Basic Energy Sciences, U.S. Department of Energy under Contract Nos. USDOE/DE-SC002183 (U. Minn.) and DE-AC02-05CH11231 (LBNL), the Swiss National Science Foundation (grant No. 200020-120007) and the seventh Framework Programme of the European Commission (Collaboration Project No. 211690), and the Hungarian Scientific Research Foundation (OTKA No. 75972).

Supporting Information Available: Supporting Information including the absolute energies of all the molecules is available free of charge at http://pubs.acs.org.This material is available free of charge via the Internet at http://pubs.acs.org.

References and Notes

(1) Evans, W. J. *Inorg. Chem.* **2007**, *46* (9), 3435–3449.
(2) Lue, C. J.; Jin, J.; Ortiz, M. J.; Rienstra-Kiracofe, J. C.; Heaven, M. C. *J. Am. Chem. Soc.* **2004**, *126*, 1812–1815.
(3) Heaven, M. C. *Phys. Chem. Chem. Phys.* **2006**, *8* (39), 4497–4509.
(4) Lozano, J. M.; Clark, D. L.; Conradson, S. D.; Den Auwer, C.; Fillaux, C.; Guilaumont, D.; Keogh, D. W.; de Leon, J. M.; Palmer, P. D.; Simoni, E. *Phys. Chem. Chem. Phys.* **2009**, *11* (44), 10396–10402.
(5) Kozimor, S. A.; Yang, P.; Batista, E. R.; Boland, K. S.; Burns, C. J.; Clark, D. L.; Conradson, S. D.; Martin, R. L.; Wilkerson, M. P.; Wolfsberg, L. E. *J. Am. Chem. Soc.* **2009**, *131* (34), 12125–12136.
(6) Wang, X. F.; Andrews, L.; Li, J.; Bursten, B. E. *Angew. Chem., Int. Ed.* **2004**, *43* (19), 2554–2557.
(7) Li, J.; Bursten, B. E.; Andrews, L.; Marsden, C. J. *J. Am. Chem. Soc.* **2004**, *126* (11), 3424–3425.
(8) Burns, J. H. *Inorg. Chem.* **1983**, *22* (8), 1174–1178.
(9) Cochran, R. G.; Tsoulfandis, N., *The Nuclear Fuel Cycle*; Analysis and Management: La Grange Park, IL, 1999.
(10) Capone, F.; Colle, Y.; Hiernaut, J. P.; Ronchi, C. *J. Phys. Chem. A* **1999**, *103*, 10899–10906.
(11) Li, J.; Bursten, B. E.; Liang, B. Y.; Andrews, L. *Science* **2002**, *295*, 2242.
(12) Infante, I.; Eliav, E.; Vilkas, M. J.; Ishikawa, Y.; Kaldor, U.; Visscher, L. *J. Chem. Phys.* **2007**, *127*, 124308.
(13) Gagliardi, L.; Heaven, M. C.; Krogh, J. W.; Roos, B. O. *J. Am. Chem. Soc.* **2005**, *127* (1), 86–91.
(14) Gagliardi, L.; Roos, B. O.; Malmqvist, P. A.; Dyke, J. M. *J. Phys. Chem. A* **2001**, *105* (46), 10602–10606.
(15) Gagliardi, L.; Roos, B. O. *Chem. Phys. Lett.* **2000**, *331* (2−4), 229–234.
(16) Roos, B. O.; Widmark, P. O.; Gagliardi, L. *Faraday Discuss.* **2003**, *124*, 57–62.
(17) Infante, I.; Visscher, L. *J. Chem. Phys.* **2004**, *121*, 5783.
(18) Han, J. D.; Goncharov, V.; Kaledin, L. A.; Komissarov, A. V.; Heaven, M. C. *J. Chem. Phys.* **2004**, *120*, 5155–5163.
(19) Han, J. D.; Kaledin, L. A.; Goncharov, V.; Komissarov, A. V.; Heaven, M. C. *J. Am. Chem. Soc.* **2003**, *125*, 7176.
(20) Santos, M. J.; Marçalo, J.; Pires de Matos, A.; Gibson, J. K.; Haire, R. G. *J. Phys. Chem. A* **2002**, *106*, 7190–7194.
(21) Santos, M. J.; Marçalo, J.; Leal, J. P.; Pires de Matos, A.; Gibson, J. K.; Haire, R. G. *Int. J. Mass Spectrom.* **2003**, *228*, 457–465.
(22) Gibson, J. K.; Haire, R. G.; Santos, M.; Marçalo, J.; Pires de Matos, A. *J. Phys. Chem. A* **2005**, *109*, 2768–2781.
(23) Gibson, J. K.; Haire, R. G.; Marçalo, J.; Santos, M.; Pires de Matos, A.; Leal, J. P. *J. Nucl. Mater.* **2005**, *344*, 24–29.
(24) La Macchia, G.; Infante, I.; Raab, J.; Gibson, J. K.; Gagliardi, L. *Phys. Chem. Chem. Phys.* **2008**, *10*, 7278–7283.
(25) Marçalo, J.; Gibson, J. K. *J. Phys. Chem. A* **2009**, *113* (45), 12599–12606.
(26) Santos, M.; Marçalo, J.; Pires de Matos, A.; Gibson, J. K.; Haire, R. G. *J. Phys. Chem. A* **2002**, *106* (31), 7190–7194.
(27) Malmqvist, P. A.; Pierloot, K.; Shahi, A. R. M.; Cramer, C. J.; Gagliardi, L. *J. Chem. Phys.* **2008**, *128* (20), 204109.
(28) Rehaman Moughal Shahi, A.; Cramer, C. J.; Gagliardi, L. *Phys. Chem. Chem. Phys.* **2009**, *11* (46), 10964−10972.

(29) Roos, B. O.; Taylor, P. R.; Siegbahn, P. E. M. *Chem. Phys.* **1980**, *48* (2), 157–173.
(30) Andersson, K.; Malmqvist, P.-Å.; Roos, B. O. *J. Chem. Phys.* **1992**, *96* (2), 1218–1226.
(31) Roos, B. O.; Lindh, R.; Malmqvist, P. A.; Veryazov, V.; Widmark, P. O. *Chem. Phys. Lett.* **2005**, *409* (4−6), 295–299.
(32) Roos, B. O.; Lindh, R.; Malmqvist, P. A.; Veryazov, V.; Widmark, P. O. *J. Phys. Chem. A* **2005**, *109* (29), 6575–6579.
(33) Karlström, G.; Lindh, R.; Malmqvist, P.-Å.; Roos, B. O.; Ryde, U.; Veryazov, V.; Widmark, P.-O.; Cossi, M.; Schimmelpfennig, B.; Neogrady, P.; Seijo, L. *Comput. Mater. Sci.* **2003**, *287*, 222–239.
(34) Roos, B. O.; Malmqvist, P. A. *Phys. Chem. Chem. Phys.* **2004**, *6* (11), 2919–2927.
(35) Malmqvist, P. A.; Roos, B. O.; Schimmelpfennig, B. *Chem. Phys. Lett.* **2002**, *357* (3−4), 230–240.
(36) Gagliardi, L. *J. Am. Chem. Soc.* **2003**, *125*, 7504–7505.
(37) Gagliardi, L. *Theor. Chem. Acc.* **2006**, *116* (1−3), 307–315.
(38) Gagliardi, L.; Cramer, C. J. *Inorg. Chem.* **2006**, *45* (23), 9442–9447.
(39) Gagliardi, L.; La Manna, G.; Roos, B. O. *Faraday Discuss.* **2003**, *124*, 63–68.
(40) Gagliardi, L.; Pyykko, P.; Roos, B. O. *Phys. Chem. Chem. Phys.* **2005**, *7* (12), 2415–2417.
(41) Gagliardi, L.; Roos, B. O. *Chem. Soc. Rev.* **2007**, *36* (6), 893–903.
(42) Infante, I.; Gagliardi, L.; Scuseria, G. E. *J. Am. Chem. Soc.* **2008**, *130* (23), 7459–7465.
(43) Infante, I.; Gagliardi, L.; Wang, X. F.; Andrews, L. *J. Phys. Chem. A* **2009**, *113* (11), 2446–2455.
(44) Infante, I.; Raab, J.; Lyon, J. T.; Liang, B.; Andrews, L.; Gagliardi, L. *J. Phys. Chem. A* **2007**, *111* (47), 11996–12000.
(45) Visscher, L.; Jensen, H. J. A.; Saue, T. *DIRAC, a relativistic ab initio electronic structure program, Release DIRAC08*; 2008.
(46) Ilias, M.; Saue, T. *J. Chem. Phys.* **2007**, *126* (6), 064102.
(47) Dyall, K. G. *J. Chem. Phys.* **1994**, *100* (3), 2118–2127.
(48) Visscher, L.; Lee, T. J.; Dyall, K. G. *J. Chem. Phys.* **1996**, *105* (19), 8769–8776.
(49) Visscher, L.; Eliav, E.; Kaldor, U. *J. Chem. Phys.* **2001**, *115* (21), 9720–9726.
(50) Dyall, K. G. *Theor. Chem. Acc.* **2004**, *112* (5−6), 403–409.
(51) Infante, I.; Severo Pereira Gomes, A.; Visscher, L. *J. Chem. Phys.* **2006**, *125*, 074301.
(52) Dunning, T. H. *J. Chem. Phys.* **1989**, *90* (2), 1007–1023.
(53) Wadt, W. R. *J. Am. Chem. Soc.* **1981**, *103* (20), 6053–6057.
(54) Dyall, K. G. *Mol. Phys.* **1999**, *96* (4), 511–518.
(55) Goncharov, V.; Heaven, M. C. *J. Chem. Phys.* **2006**, *124* (6), 7.
(56) Heaven, M. C.; Goncharov, V.; Steimle, T. C.; Ma, T. M.; Linton, C. *J. Chem. Phys.* **2006**, *125*, 204314.
(57) Paulovic, J.; Gagliardi, L.; Dyke, J. M.; Hirao, K. *J. Chem. Phys.* **2005**, *122*, 144317.
(58) Goncharov, V.; Kaledin, L. A.; Heaven, M. C. *J. Chem. Phys.* **2006**, *125* (13), 8.
(59) Denning, R. G.; Norris, J. O. W.; Brown, D. *Mol. Phys.* **1982**, *46* (2), 287–323.
(60) Denning, R. G.; Norris, J. O. W.; Brown, D. *Mol. Phys.* **1982**, *46* (2), 325–364.
(61) Matsika, S.; Pitzer, R. M. *J. Phys. Chem. A* **2000**, *104* (17), 4064–4068.
(62) Rauh, E. G.; Ackermann, R. J. *J. Chem. Phys.* **1974**, *60* (4), 1396–1400.
(63) Capone, F.; Colle, J. Y.; Hiernaut, J. P.; Ronchi, C. *J. Phys. Chem. A* **2005**, *109*, 12054–12058.
(64) Kovacs, A.; Konings, R. J. M.; Raab, J.; Gagliardi, L. *Phys. Chem. Chem. Phys.* **2008**, *10* (8), 1114–1117.
(65) Notter, F. P.; Dubillard, S.; Bolvin, H. *J. Chem. Phys.* **2008**, *128* (16), 12.

JP1016328